Electronic Supplementary Material (ESI) for Journal of Materials Chemistry A.

The adaptive kinetic Monte Carlo code DL_AKMC can be found at http://ccpforge.cse.rl.ac.uk/gf/project/kmc/

1 Initial starting arrangement

We have investigated the effect of the initial starting arrangement of dopant cations and anion vacancies on the ionic conductivities of YSZ, CSZ, SDC and GDC over the same dopant concentrations used in the paper. The configurations used were; 'associated', where the anion vacancies are nearest neighbours to the dopant cations; 'unassociated', where dopant cations and anion vacancies were separated by a minimum of 4.5Å; 'random', where the dopant cations and anion vacancies are randomly distributed through the material. The ionic conductivities of each of these arrangements at each dopant concentration was determined after adaptive kinetic Monte Carlo simulation (using a procedure identical to that in the paper) and representative results for YSZ are shown in Figure 1.

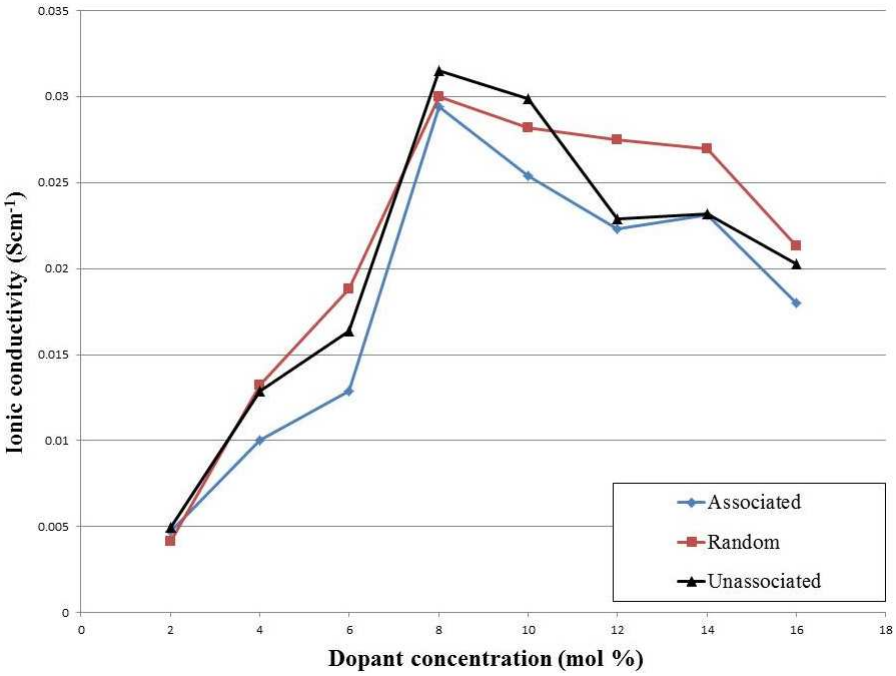

Figure 1 Ionic conductivities for YSZ from the three different starting configurations.

From Figure 1 it can be seen that the general form of the ionic conductivity versus dopant concentration curve is maintained regardless of the starting configuration, and the magnitude of the ionic conductivity does not vary dramatically between arrangements. The other materials investigated exhibited similar closeness in magnitude and form of their conductivity curves.

2 Radial Distribution Function

For further interest we present in Figure 2 the radial distribution function (RDF) for Gd-Gd in 10 mol% GDC.

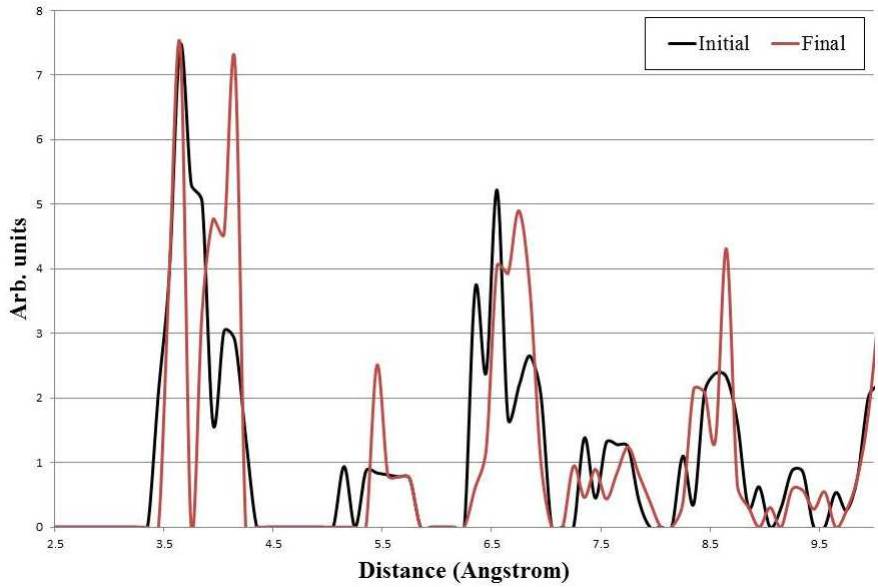

Figure 2 Radial distribution functions at the beginning of the simulation (initial) and at the end (final) for Gd-Gd in the 'random' configuration for 10 mol% GDC.

Figure 2 illustrates that the Gd-Gd distance tends to decrease over the course of the simulation, leading to possible Gd clustering. This effect is seen to a greater or lesser extent regardless of initial configuration, but does not appear to affect the ionic conductivity significantly.

3 Potential Parameter Verification

Tables 1, 2 and 3 show values of representative physical parameters calculated using the potential set listed in the main text, along with values for related binary oxide materials for comparison.

Table 1 Calculated and experimental bulk properties of representative binary oxides.

Property	ZrO_2		CeO_2		$LaCoO_3$		CaO	
	Calc.	Expt. [1,2]	Calc.	Expt. [3–5]	Calc.	Expt. [6,7]	Calc.	Expt. [8,9]
Lattice parameter, a (Å)	5.127	5.127	5.386	5.406	3.839	3.823	4.812	4.810
Bulk modulus (GPa)	278	185	263	236	255	150	136	114
Elastic constant, C_{11} (GPa)	596	401	521	403	410	-	211	223

Table 2 Calculated and experimental bulk properties of representative binary oxides.

Property	SrO		Y_2O_3		Gd_2O_3		Sm_2O_3	
	Calc.	Expt. [10,11]	Calc.	Expt. [12]	Calc.	Expt. [13]	Calc.	Expt. [14]
Lattice parameter, a (Å)	5.160	5.162	10.362	10.603	10.435	10.819	10.923	10.928
Bulk modulus (GPa)	102	91	184	150	196	188	163	149
Elastic constant, C_{11} (GPa)	155	170	284	224	294	-	244	-

Table 3 Calculated and related experimental bulk properties of 10 mol % doped zirconias, 15 mol % doped cerias and 50 mol % doped LCO.

Property	ZrO_2	10-YSZ	10-CSZ	CeO_2	15-GDC	15-SDC	$LaCoO_3$	50-LSCO
	Expt. [1,2]	Calc.	Calc.	Expt. [3–5]	Calc.	Calc.	Expt. [6,7]	Calc.
Lattice parameter, a (Å)	5.127	5.158	5.173	5.406	5.412	5.420	3.823	3.873
Bulk modulus (GPa)	185	217	211	236	236	232	150	196
Elastic constant, C_{11} (GPa)	401	514	441	403	449	443	-	291

4 Migration pathway

Included for interest is a representative anion vacancy migration pathway along the (100) direction in 20 mol % GDC (Figure 3). The majority of diffusion occurs in this direction due to the presence of the applied field. In this example, the activation barrier was found to be 0.27 eV.

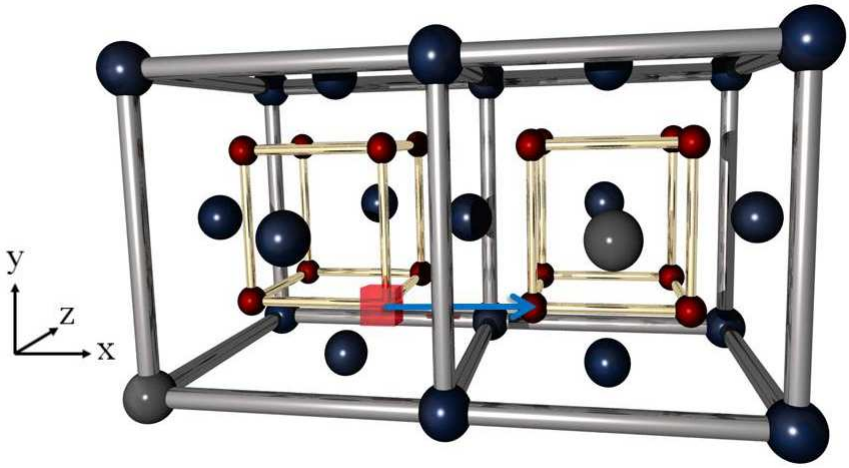

Figure 3 Representative anion vacancy migration pathway along the (100) direction in 20 mol % GDC. The large, blue atoms are Ce, the large, grey atoms are Gd, and the smaller red atoms are oxygen. The oxygen vacancy is shown as a red transparent cube. Not all atoms included in the simulation are shown here.

References

[1] A. Rabenau. *Z. Anorg. Allgne. Chem.*, 288:221, 1956.

[2] P.J. Botha, J.C.H. Chiang, J.D. Comins, P.M. Mjwara, and P.E. Ngoepe. *J. Appl. Phys.*, 73:7268, 1993.

[3] S.J. Duclos, Y.K. Vohra, A.L. Ruoff, A. Jayaraman, and G.P. Espinosa. *Phys. Rev. B*, 38:7755, 1988.

[4] L. Gerward and J. Staun Olsen. *Powder Diffr.*, 8:127, 1993.

[5] A. Nakajima, A. Yoshihara, and M. Ishigma. *Phys. Rev. B*, 50:13297, 1994.

[6] M.S. Islam. *Solid State Ionics*, 154:75, 2002.

[7] T. Vogt, J.A. Hriljac, N.C. Hyatt, and P. Woodward. *Phys. Rev. B*, 67:140401, 2003.

[8] M.J. Mehl, R.J. Hemley, and L.L. Boyer. *Phys. Rev. B*, 33:8685, 1986.

[9] Z.P. Chang and E.K. Graham. *J. Phys. Chem. Solids*, 38:1355, 1977.

[10] L.-G. Liu and W.A. Bassett. *J. Geophys. Res.*, 77:4934, 1972.

[11] T.J. Ahrens. *Mineral Physics & Crystallography: A Handbook of Physical Constants*. American Geophysical Union, USA, 1995.

[12] J.W. Palko, W.M. Kriven, S.V. Sinogeikin, J.D. Bass, and A. Sayir. *J. Appl. Phys.*, 89:7791, 2001.

[13] F.X. Zhang, M. Lang, J.W. Wang, and R.C. Becker, U. Ewing. *Phys. Rev. B*, 78:064114, 2008.

[14] S. Jiang, J. Liu, C. Lin, X. Li, and Y. Li. *J. Appl. Phys.*, 113:113502, 2013.